PERGAMON

International Journal of Heat and Mass Transfer 44 (2001) 389–397

International Journal of HEAT and MASS TRANSFER

www.elsevier.com/locate/ijhmt

Mixed convection in an unequally heated loop: steady solutions

Min-Joon Kim*, Yong-Bum Lee, Yong-Kyun Kim, Byoung-Hae Choi, Ho-Yun Nam

KALIMER Sodium Experimental Technology Laboratory, Korea Atomic Energy Research Institute, Yousiong P.O. Box 105, Taejon 305-600, South Korea

Received 31 August 1999; received in revised form 3 March 2000

Abstract

We consider a one-dimensional mixed convection of liquid metal with forced circulation and unequal heating. The steady solution of the corresponding heat equation with proper boundary conditions is obtained analytically. The solution shows formation of a local circulation loop by unequal heating and deformation of the circulation loop by the forced circulation. It is also found that the heat transfer characteristics are almost independent of the unequal heating condition, although the deformation occurs more easily for a more symmetric case.

1. Introduction

Convection heat transfer has been usually studied in natural convection dominant region or in forced convection dominant region. However, in nature, there are many phenomena that cannot be explained by either limit. In such phenomena, buoyancy effect that induces natural convection and externally imposed flow condition that results in forced convection, both participate in heat transfer. Usually, this kind of convection is called 'mixed convection.'

So far, there have been many studies on mixed convection [1,2], but the phenomena are so complicated that the fundamental features of mixed convection heat transfer are not fully known yet. In this paper, we consider a simple mixed convection system that can be treated one-dimensionally. Even though mixed convection phenomena are usually two- or three-dimensional, we expect that the one-dimensional approach may give an insight for complex mixed convection phenomena.

The idea of the target system is obtained from heat transfer in the core of a nuclear reactor (Fig. 1) [3,4]. In the core, generally, the heat generation rate is not uniform, which may induce natural convection in the core. There also exists global circulation between the core and a heat exchanger. When the two effects, the non-uniform heating and the global circulation, are comparable, the heat transfer should be treated as a mixed convection phenomenon.

To simulate the heat transfer in the core of a nuclear reactor, we design a simple model system (Fig. 2). It is composed of a circulation loop with an inlet through which flow is provided externally and an outlet through which the provided flow outflows. The target system can also be considered as two geometrically symmetric vertical channels whose inlets and outlets coincide respectively. The non-uniform heating in the

* Corresponding author. Tel.: +82-42-868-2069; fax: +82-42-868-8739.

E-mail address: mjkim@etri.re.kr (M.-J. Kim).

0017-9310/01/$ - see front matter
PII: S0017-9310(00)00111-3

Nomenclature

A	cross-sectional area of the channel
C_p	specific heat
$\vec{g}$	gravitational acceleration
l	half-height of the channel
p	pressure
Pe	Péclet number
$Q(X)$, $q(x)$	dimensional and dimensionless heat input distribution functions
Q_i, q_i	dimensional and dimensionless heat inputs (i = L, R, h, tot)
r	dimensional radial axis
T	dimensional temperature
t	time
U, u	dimensional and dimensionless average flow velocities
X, x	dimensional and dimensionless axial axes

Greek symbols

α	heat diffusivity
β	coefficient of expansion
μ	viscosity
ρ	density of fluid
ϕ	dimensional azimuthal axis

Subscripts

ext	given externally
h	heater
L	left channel
R	right channel
r	flow reversal
ref	reference
tot	total

core is simply represented with two heaters of different powers installed at the centers of the left and the right channels. The strengths are denoted by Q_L and Q_R for the left and the right, respectively. U_{ext} denotes the velocity of the fluid provided at the inlet. Heights of both the channels are $2l$. Although this system is a crude approximation to the real one, we can study the qualitative nature of the mixed convection heat transfer. A similar approach can be found in the study of Rayleigh–Bernard convection [5].

Qualitative predictions for the asymptotic cases ($U_{ext}\to 0$ and $U_{ext}\to\infty$) can be made. When the buoyancy effect caused by the unequal heating dominates (natural circulation limit), a circulation loop forms, as shown in Fig. 3(a). Without loss of generality, we assumed $Q_L > Q_R$. However, when the provided flow dominates (forced circulation limit), the circulation loop disappears and fluid flows upwards in both channels (Fig. 3(b)). Existence of the flow reversal point may affect heat transfer and is usually expected to increase the system temperature, which is undesirable considering safety.

In this paper, the formation and deformation of the circulation loop and heat transfer are studied quantitatively and analytically. Especially, we will focus on the steady solutions of the liquid metal loop. The

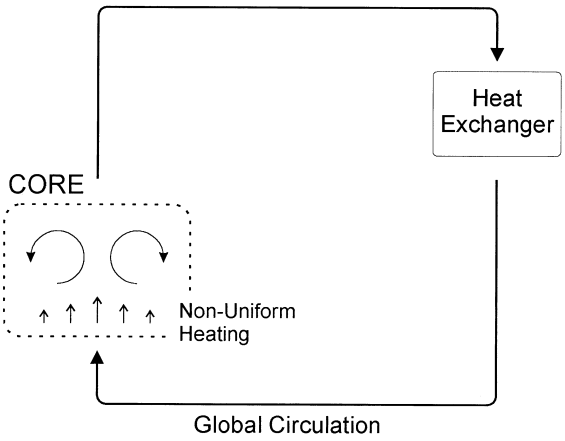

Fig. 1. Heat transfer in a nuclear reactor. Natural convection induced by the non-uniform heating in the core and the global circulation between the core and a heat exchanger compete with each other and play major roles in the heat transfer.

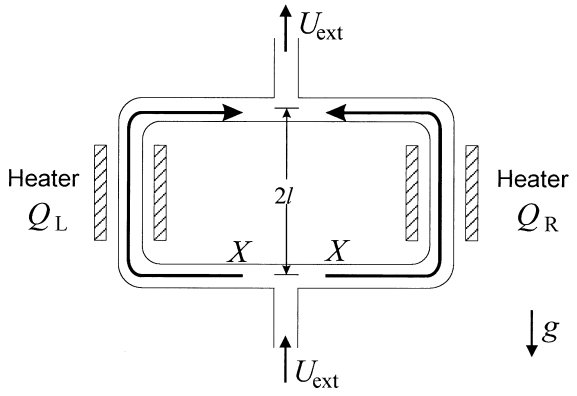

Fig. 2. The target system is composed of two vertical channels with heat sources at the centers of the channels. The system is geometrically symmetric but the heat source strengths are different.

model system is similar to the thermosyphon with throughflow [6–9], especially Mertol's thermosyphon [7]. But, there are two major differences. One is symmetry. While Mertol's thermosyphon is symmetric with respect to the horizontal axis and there is no preferred flow direction without throughflow, our system has a preferred flow direction due to the unequal heating. The other difference is the working fluid. For liquid metal, the conduction effect cannot be neglected whereas Mertol neglected it.

2. Formulation

For heat transfer phenomena, governing equations are usually composed of the continuity equation (mass conservation),

$$\frac{\partial \rho}{\partial t} + \nabla \cdot \left(\rho \vec{U}\right) = 0, \tag{1}$$

the momentum equation (Navier–Stokes' equation),

$$\rho\left(\frac{\partial \vec{U}}{\partial t} + \vec{U} \cdot \nabla \vec{U}\right) = -\nabla p + \mu \nabla^2 \vec{U} + \rho \vec{g}, \tag{2}$$

the energy equation (heat equation),

$$\frac{\partial T}{\partial t} + \vec{U} \cdot \nabla T = \alpha \nabla^2 T + \frac{Q}{\rho C_p A}, \tag{3}$$

and boundary conditions. Here, $\vec{U}$, p, T, A and Q are velocity, pressure, temperature, cross-sectional area and heat distribution function, respectively. And ρ, μ, $\vec{g}$, α, and C_p are density, viscosity, gravitational acceleration, heat diffusivity, and specific heat, respectively. Time axis is t.

For the system under consideration, the coordinates are set as shown in Fig. 2. In both the channels, the axial axes are denoted by X and the radial and azimuthal axes by (r, ϕ). For each channel, the direction of the axial axis X is from the inlet to the outlet, individually.

For simplicity, we introduce several assumptions. The most important assumption is that the flow in the loop is one-dimensional except at the inlet and the outlet. Since our focus is on the heat transfer in axial direction, this assumption is efficient unless the diameter of the channel is comparable to or larger than the length.

We employ Boussinesq approximation and write the density as

$$\rho = \rho_{\text{ref}}(1 - \beta(T - T_{\text{ref}})), \tag{4}$$

where β is the coefficient of expansion and ρ_{ref} is the density at $T = T_{\text{ref}}$. We assume no pressure drop, which is found valid except near the flow reversal point. We also assume a volumeless heat source, zero horizontal lengths of the channels and no heat loss to surroundings for simplicity.

Under the one-dimensional flow assumption, the governing equations can be simplified by averaging the three-dimensional equations with respect to cross-section plane, i.e. (r, ϕ) plane. Especially, the continuity equation can be rewritten with the average axial velocity $\langle U \rangle$

$$\frac{\partial \langle U \rangle}{\partial X} = 0, \tag{5}$$

except at the inlet and the outlet. Eq. (5) implies that the average velocity is constant throughout each channel, so that

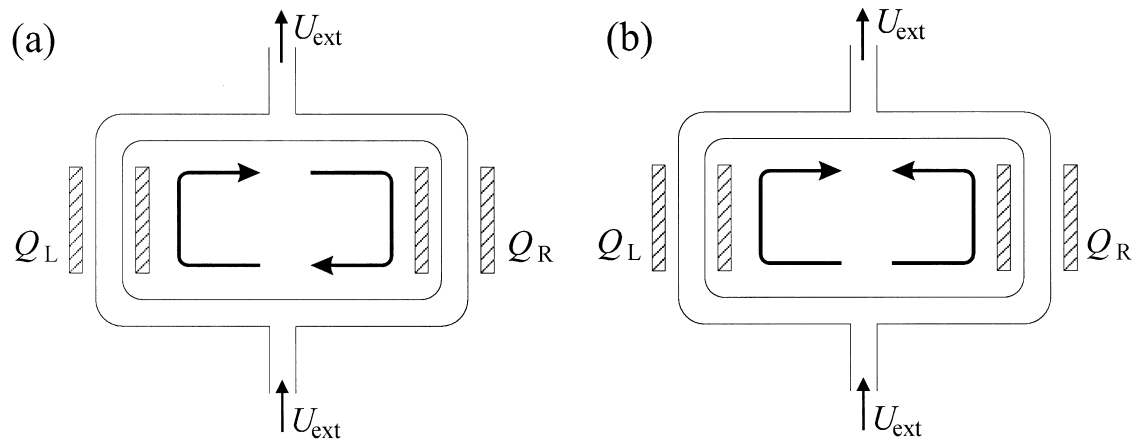

Fig. 3. Two prototypes for flow directions in the channels. (a) A circulation loop is formed. (b) The circulation loop is deformed and the flow directions are all upwards.

$$\langle U\rangle = \begin{cases} U_{\mathrm{L}} & \text{for the left channel,} \\ U_{\mathrm{R}} & \text{for the right channel,} \end{cases} \tag{6}$$

where U_{L} and U_{R} are constants. Recall that the test loop is geometrically symmetric, so the cross-sectional areas are all same.

For steady solutions, the momentum equation implies force balance. For this system, force balance can be replaced by buoyancy balance assuming no pressure drop, which is written as

$$\int \rho_{\mathrm{L}}\vec{g}\,\mathrm{d}X = \int \rho_{\mathrm{R}}\vec{g}\,\mathrm{d}X, \tag{7}$$

where $\rho_{\mathrm{L}}(X)$ and $\rho_{\mathrm{R}}(X)$ are the densities in the left and right channels, respectively. With temperatures, Eq. (7) becomes

$$\int_0^{2l} T_{\mathrm{L}}\,\mathrm{d}X = \int_0^{2l} T_{\mathrm{R}}\,\mathrm{d}X. \tag{8}$$

where T_{L} and T_{R} are the temperatures in the left and right channels.

With volumeless heat source assumption, Q is expressed with Dirac's delta function:

$$Q(x) = Q_{\mathrm{h}}\delta(X - X_{\mathrm{h}}), \tag{9}$$

where Q_{h} is the heat source strength and X_{h} is the heat source location.

The boundary conditions must be considered carefully. First, temperature is continuous everywhere, including at the inlet, at the outlet, and at the heat source positions. And the first derivative of temperature, $\mathrm{d}T/\mathrm{d}X$ is also continuous everywhere except at the inlet and at the heat source positions. Note that $\mathrm{d}T/\mathrm{d}X$ is continuous at the outlet because there are no external constraints on temperature at the outlet. In other words, flows from both channels are mixed together freely at the outlet. The continuity and discontinuity are mainly due to conduction. Similar examples can be found in the study of shock waves [10].

For convenience, we locate the origin of temperature at the inlet, so that $T(X = 0) = 0$. This is mathematically valid, if appropriate values are chosen for the physical quantities. Note that this shift of origin implies that there is a heat reservoir at the inlet.

Let us introduce dimensionless variables, u, x, θ, and q:

$$(U, U_{\mathrm{L}}, U_{\mathrm{R}}) = U_{\mathrm{ext}}(u, u_{\mathrm{L}}, u_{\mathrm{R}}), \tag{10}$$

$$X = lx, \tag{11}$$

$$(T, T_{\mathrm{L}}, T_{\mathrm{R}}) = T_0(\theta, \theta_{\mathrm{L}}, \theta_{\mathrm{R}}), \tag{12}$$

$$(Q_{\mathrm{L}}, Q_{\mathrm{R}}) = Q_{\mathrm{tot}}(q_{\mathrm{L}}, q_{\mathrm{R}}), \tag{13}$$

where

$$T_0 = \frac{Q_{\mathrm{tot}}}{\rho C_p A U_{\mathrm{ext}}}, \tag{14}$$

$$Q_{\mathrm{tot}} = Q_{\mathrm{L}} + Q_{\mathrm{R}}, \tag{15}$$

$$Pe = \frac{lU_{\mathrm{ext}}}{\kappa}. \tag{16}$$

Usually, Pe is called the Péclet number. With this nondimensionalization, the inlet position is $x = 0$ and the outlet, $x = 2$. The heat sources are located at $x = 1$. Remember that we assumed zero horizontal lengths.

The Eqs. (1), (3), (6), (8), and (15) are given in their nondimensional form in Eqs. (17)–(21), respectively.

$$u_{\mathrm{L}} + u_{\mathrm{R}} = 1, \tag{17}$$

$$u_i\frac{\mathrm{d}\theta_i}{\mathrm{d}x} = \frac{1}{Pe}\frac{\mathrm{d}^2\theta_i}{\mathrm{d}x^2} + q_i\delta(x - 1), \tag{18}$$

$$\langle u\rangle = \begin{cases} u_{\mathrm{L}} & \text{for the left channel,} \\ u_{\mathrm{R}} & \text{for the right channel,} \end{cases} \tag{19}$$

$$\int_0^2 \theta_{\mathrm{L}}\,\mathrm{d}x = \int_0^2 \theta_{\mathrm{R}}\,\mathrm{d}x, \tag{20}$$

$$q_{\mathrm{L}} + q_{\mathrm{R}} = 1, \tag{21}$$

for $i = \mathrm{L}, \mathrm{R}$.

3. Solutions

3.1. Solution of the heat equation

For solutions of the full system, first, it is convenient to find a solution of the one-dimensional heat equation,

$$u_i\frac{\mathrm{d}\theta_i}{\mathrm{d}x} = \frac{1}{Pe}\frac{\mathrm{d}^2\theta_i}{\mathrm{d}x^2} + q_i\delta(x - 1), \tag{22}$$

with boundary conditions at the inlet,

$$\theta_i(x = 0) = 0, \tag{23}$$

and at the outlet,

$$\theta_i(x = 2) = \Delta\theta = \theta_{\mathrm{out}} - \theta_{\mathrm{in}}, \tag{24}$$

for $i = \mathrm{L}, \mathrm{R}$. In addition, θ_i is continuous everywhere and $\mathrm{d}\theta_i/\mathrm{d}x$ is continuous except at $x = 1$, the heat

source position. Here, θ_{in} and θ_{out} are the inlet and outlet temperatures, respectively.

The solution of the heat equation has the form of

$$\theta = AE_i^x + B, \tag{25}$$

except for $u_i = 0$, where

$$E_i = e^{u_i Pe}. \tag{26}$$

Because heat transfer for the $u_i = 0$ case can be studied as the limit case of $u_i \to 0$, it will not be treated as a special case.

Integrating the heat equation from 1^- to 1^+, we have the following equation as the jump condition at the heat source position:

$$\left.\frac{d\theta_i}{dx}\right|_{1^+} - \left.\frac{d\theta_i}{dx}\right|_{1^-} = -q_i Pe. \tag{27}$$

To solve the equation more easily, we introduce a new variable $\theta_{h,i}$ such that

$$\theta_i(x = 1) = \theta_{h,i}, \tag{28}$$

for $i = L, R$.

Considering the boundary conditions, the solution is found as

$$\theta_i = \begin{cases} \theta_{h,i}\left(E_i^x - 1\right)/(E_i - 1) & \text{for } 0 < x < 1, \\ \theta_{h,i} & \text{for } x = 1, \\ \left(\Delta\theta - \theta_{h,i}\right)\left(E_i^{x-1} - 1\right)/(E_i - 1) + \theta_{h,i} & \text{for } 1 < x < 2. \end{cases} \tag{29}$$

Note that the solution of the full system satisfies the temperature continuity conditions at the inlet and at the outlet automatically from the boundary conditions, Eqs. (23) and (24).

With the jump condition at $x = 1$, we can eliminate $\theta_{h,i}$:

$$\theta_{h,i} = \left[\Delta\theta - \frac{q_i}{u_i}(1 - E_i)\right]/(1 + E_i), \tag{30}$$

for $i = L, R$.

3.2. Solution and its characteristics

Now, the unknowns are u_L, u_R, and $\Delta\theta$ for the solution of the full system, and the parameters are Pe and q_L (or q_R). Let us consider the other conditions left, buoyancy balance, continuity of $d\theta/dx$ at the outlet, and mass conservation.

First, from the continuity of $d\theta/dx$ in Eq. (29) at the outlet, after a little algebra, we have

$$\Delta\theta = \left[q_L \frac{E_L}{E_L + 1} + q_R \frac{E_R}{E_R + 1}\right] \Bigg/ \left[\frac{u_L E_L^2}{E_L^2 - 1} + \frac{u_R E_R^2}{E_R^2 - 1}\right]. \tag{31}$$

And from the buoyancy balance in Eq. (20), we have

$$\Delta\theta = \left[\frac{Q_L}{u_L}\frac{E_L - 1}{E_L + 1} - \frac{Q_R}{u_R}\frac{E_R - 1}{E_R + 1}\right] \Bigg/ \left[\left(\frac{1}{u_R Pe} - \frac{1}{u_L Pe}\right) - 2\left(\frac{1}{E_R^2 - 1} - \frac{1}{E_L^2 - 1}\right)\right]. \tag{32}$$

Comparing Eqs. (31) and (32), with the mass conservation constraint, $u_L + u_R = 1$, we can find a solution. Several examples are shown in Fig. 4. The solid lines are the curves for the continuity equation (31) and the dashed lines are for the balance equation (32). The intersection point of the two curves is the solution. As shown in several examples in Fig. 4, there exists one solution for each case. And the solutions are found to be linearly stable.

The curves of $d\theta/dx$ continuity, the solid lines, have a maximum near $u_R = 1/2$. As Pe increases, the maximum value increases and converges to 1. It should be noted that the maximum value is still less than 1, which corresponds to the heat transfer rate for the forced convection limit. It is also found that the curve becomes flat around the maximum as Pe becomes larger. We think that the flatness is closely related to the heat transfer characteristics. It will be discussed later. For the same Pe values, the curves seem almost the same even for different q_R values. But actually, the curves become more symmetric (with respect to $u_R = 1/2$) as the heating condition becomes symmetric even though the differences are small.

The curves of the force balance, the dashed lines, diverge near $u_R = 1/2$. The divergence appears because the buoyant force is hardly compensated with equal flow distribution ($u_R = u_L = 1/2$). For small Pe (Fig. 4(a), (c), (e)), the curve is nearly anti-symmetric with respect to $u_R = 1/2$. However, for large Pe (Fig. 4(b), (d), (f)), the left segment of the curve changes its shape and appears to have a local minimum. For the case that the minimum exists, the solution lies between the minimum and $u_R = 1/2$.

For $q_R = 0.25$ ($q_L = 0.75$) and $Pe = 1.0$ (Fig. 4(a)), for the solution, u_R is found to be negative, which implies that a local circulation loop forms (Fig. 3(a)). For this case, the temperature profile is shown in Fig. 5(a). The solid line is for θ_L and the dashed for θ_R. For $q_R = 0.25$ and $Pe = 7.0$, for the solution, u_R is found to be positive, which implies that fluid flows from the inlet to the outlet in both

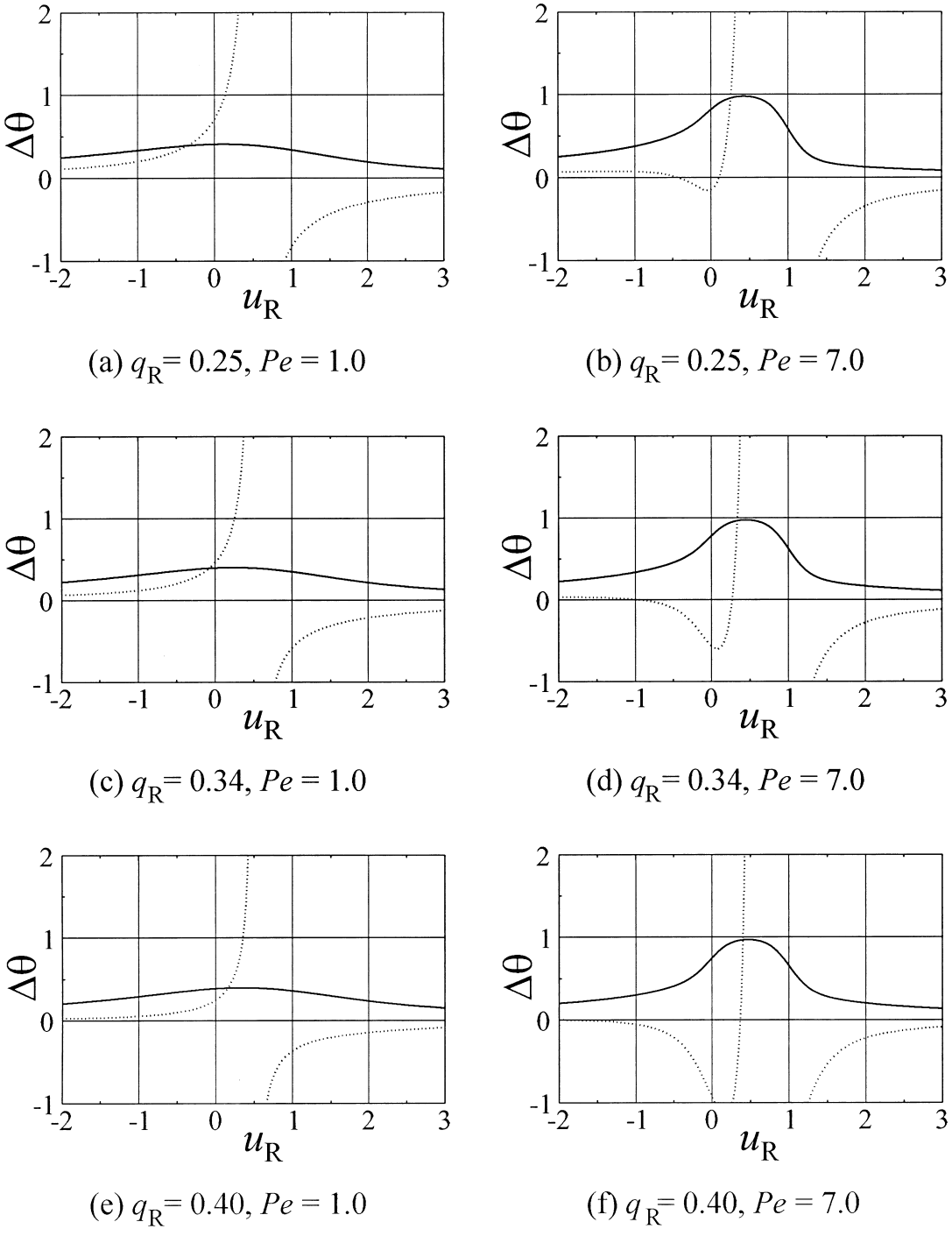

Fig. 4. Temperature differences obtained from the $d\theta/dx$ continuity constraint (solid lines) and the force balance constraint (dashed lines). The intersection point is the solution: (a) $q_R = 0.25$ and $Pe = 1.0$, (b) $q_R = 0.25$ and $Pe = 7.0$, (c) $q_R = 0.34$ and $Pe = 1.0$, (d) $q_R = 0.34$ and $Pe = 7.0$, (e) $q_R = 0.40$ and $Pe = 1.0$, (f) $q_R = 0.40$ and $Pe = 7.0$.

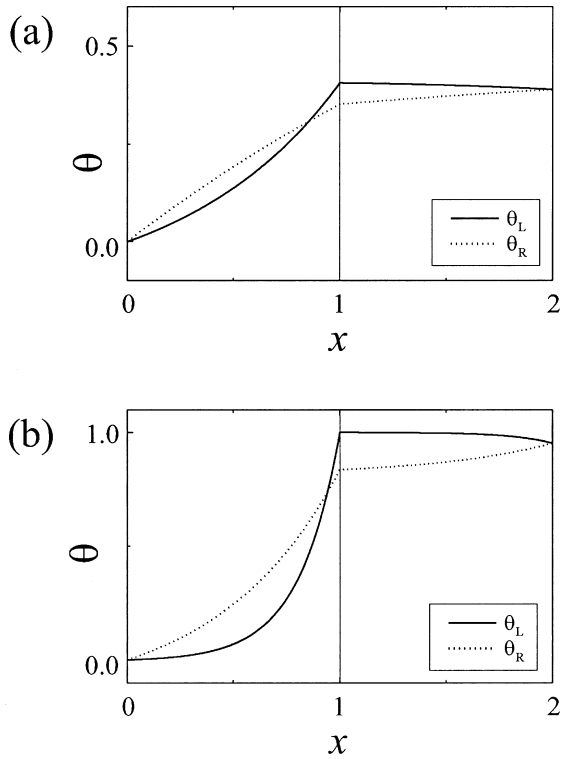

Fig. 5. Temperature profiles: the solid line is for θ_L and the dashed for θ_R. (a) $q_R = 0.25$ and $Pe = 1.0$, (b) $q_R = 0.25$ and $Pe = 7.0$.

channels. For this case, the temperature profile is shown in Fig. 5(b). The major difference between the two temperature profiles is the slope variations. For the other q_R values, the qualitative features are the same as those for $q_R = 0.25$.

Flow distribution by the buoyant force is studied. The relations between u_R and Pe are given in Fig. 6

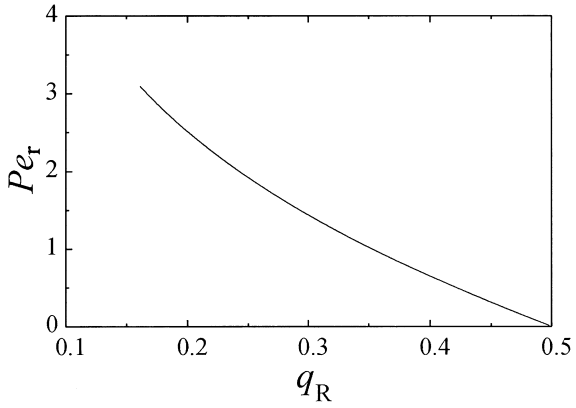

Fig. 7. Flow reversal condition ($u_R = 0$).

for different q_Rs. As Pe increases, u_R converges to a certain value, which is large for large q_R. In Fig. 6, we can find the flow reversal conditions where u_R changes its sign. The flow reversal implies deformation of the local circulation loop formed by unequal heating. As q_R approaches 1/2, for a more symmetric case, the local circulation loop becomes easy to disappear, that is, flow reversal occurs for small Pe. The detailed feature is shown in Fig. 7, where the flow reversal condition, say Pe_r, is plotted with respect to q_R.

Heat transfer can be characterized with $\Delta\theta$. In Fig. 8, $\Delta\theta$ is plotted with respect to Pe for the different q_Rs. It is hard to identify the curves in Fig. 8(a), so a magnified figure is given in Fig. 8(b). As Pe increases, $\Delta\theta$ increases and soon converges to $\Delta\theta = 1$, the forced circulation limit. For a large q_R, the convergence of $\Delta\theta$ occurs faster than for small q_R. The convergence of the heat transfer characteristics is closely related to the flatness of $d\theta/dx$ continuity curve. For a sufficiently large Pe, the continuity curve has a large plateau

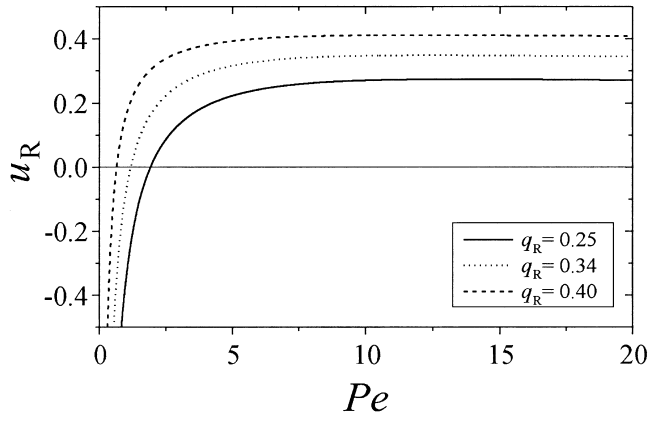

Fig. 6. Relation between u_R and Pe.

around $u_R = 1/2$, whose height is nearly equal to 1. Therefore, $\Delta\theta$ of the intersection point is approximately 1, even though u_R converges to different values for different heating conditions.

For small Pe, $\Delta\theta$ is small compared to that of the forced circulation limit. The small $\Delta\theta$ means that the heat supply from the sources transfers out faster. In other words, the heat transfer characteristics are enhanced by decreasing Pe, even though the real temperature difference, ΔT increases. One of the main reasons for the enhancement is the relative growth of conduction effect that is negligible for large Pe. The present results also show that $\Delta\theta$ does not diverge as Pe goes to 0 or near the flow reversal point ($u_R = 0$) while it might be expected. The divergence of $\Delta\theta$ is thought to be avoided by the smoothing effect of conduction.

As shown in Fig. 8, the heat transfer characteristics seem almost independent of q_R for all ranges including the region near the flow reversal point. The heat transfer rates exhibit small differences only near the flow reversal point (the flow reversal condition for $q_R = 0.25$, $Pe_{r,\,0.25}$ is shown in Fig. 8 for comparison), where conduction effect is comparable to effect of convection. The differences can be neglected for several

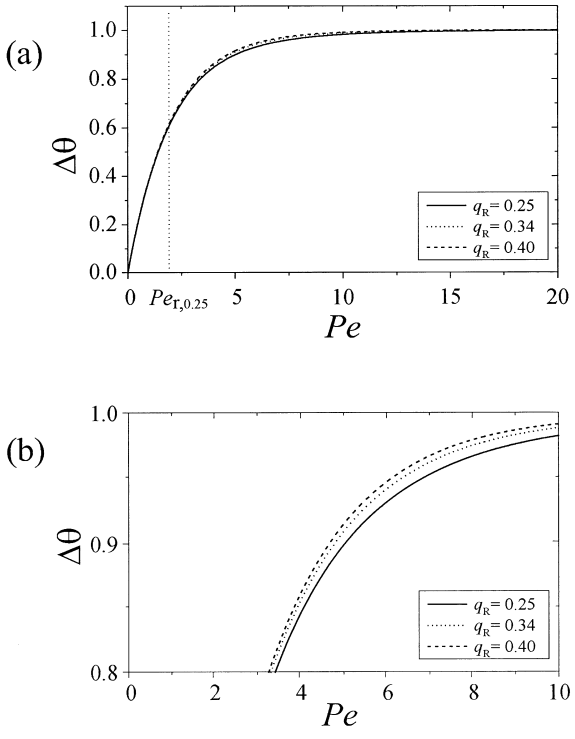

Fig. 8. Relation between $\Delta\theta$ and Pe. Because of the difficulty in identification of the curves, a magnified figure is given in (b). The flow reversal condition for $q_R = 0.25$, $Pe_{r,\,0.25}$ is shown for comparison.

systems from the practical point of view. For example, in the decay heat removal of PRISM, Pe is about a few hundred or more [3].

Heat transfer characteristics are associated with flow redistribution caused by buoyant effect due to unequal heating. Dramatically, in this system, the flow redistribution has tendencies to compensate the effect of the unequal heating and to regularize the heat transfer, which makes the differences unnoticeable. The reason for the independence can be found in the existence of the flat region on the $d\theta/dx$ continuity curve. If the solution is found in the flat region, the consequent heat transfer exhibits almost the same feature, even though different unequal heating condition, of course, causes different flow distribution. Since the larger Pe is, the wider the flat region becomes, the effect of unequal heating is harder to detect for large Pe.

Let us recall the origin of the curve that has the flat region. The curve was derived from $d\theta/dx$ continuity at the outlet. This implies that the outlet temperature free constraint is one of the major key-points for the flow redistribution and heat transfer. For detailed mechanism, more studies will be required.

Available experimental results [4] are shown in Fig. 9 for comparison. Qualitative features of the experimental results agree with the analytical results, especially the independence from unequal heating condition, although the analytical results underestimate the flow reversal point. The quantitative disagreement near the flow reversal point seems to result from no pressure drop assumption.

4. Summary and further researches

Competition of forced circulation and buoyancy effect induced by unequal heating was investigated analytically. The system was simplified and treated as a one-dimensional loop. For the governing equation, one-dimensional heat equations with proper boundary conditions were considered. The steady solution for liquid metal was found from simultaneous satisfaction of the continuity condition and the buoyancy balance.

A survey of solutions showed that flow reversal, that is, deformation of a local circulation loop formed by unequal heating, occurs at certain values of Pe, say Pe_r, which was found to be small for nearly symmetric cases. For small Pe, for the natural circulation limit and even near the flow reversal point, enhancement of heat transfer characteristics was found, which is due to increment of conduction effect. Moreover, the heat transfer characteristics are found to be almost independent of the unequal heating condition, which is achieved by self-redistribution of flow and closely related to the outlet temperature free constraint. From a comparison of the analytical results with experimental

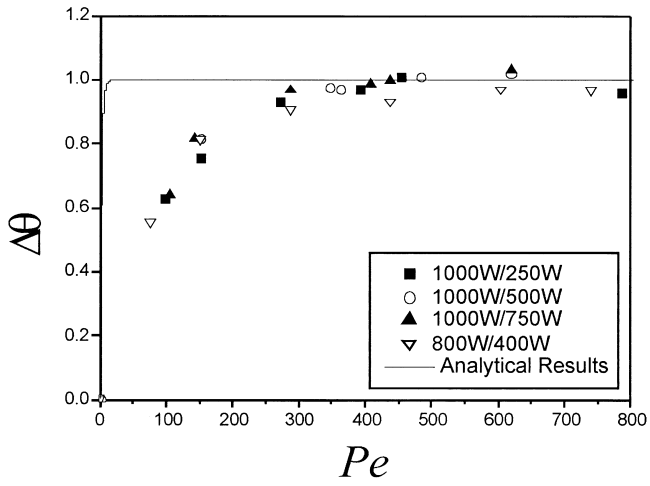

Fig. 9. Heat transfer characteristics: the analytical results and the experimental results.

results, we can find that the heat transfer characteristics exhibit the same qualitative features.

For the system we have considered here, the outlet temperature was obtained from some constraints. But sometimes, the outlet temperature can be fixed. For this case, the outlet temperature becomes a parameter and more interesting heat transfer phenomena may be found. For example, in a recent report [3], heat transfer was announced to be sensitive to the outlet temperature. The stabilization by flow redistribution may not be found in those systems. More studies are required for the flow redistribution mechanism.

Acknowledgements

This work has been supported by the Nuclear R&D Program, Ministry of Science and Technology.

References

[1] A. Bhattacharyya, Effect of Buoyancy on Forced Convection Heat Transfer in Vertical Channels, AE-176, Aktiebolaget Atomenergi, Stockholm/Sweden, 1965.

[2] T.Y. Chu, T.S. Chen, Fundamentals of Mixed Convection 1994, ASME, 1994.

[3] Y.-B. Lee, M.-J. Kim, S.-K. Choi, Y.-K. Kim, H.-Y. Nam, Heat transfer behavior in a sodium loop due to inlet flow change: experiments and numerical calculations, in: J.S. Lee (Ed.), Proceedings of the Eleventh International Heat Transfer Conference, vol. 6, Taylor and Francis, Philadelphia, PA, 1998, pp. 57–62.

[4] M.-J. Kim, Y.-B. Lee, S.-K. Choi, Y.-K. Kim, H.-Y. Nam, Formation and deformation of local convection due to non-uniform heating and fluid injection, in: Proceedings of the Sixth International Conference on Nuclear Engineering, ASME, 1998, p. 6489.

[5] J.A. Yorke, E.D. Yorke, Chaotic behavior and fluid dynamics, in: H.L. Swinney, J.P. Gollub (Eds.), Hydrodynamic Instabilities and the Transition to Turbulence, Springer-Verlag, Berlin, 1985, pp. 77–95.

[6] Y. Zvirin, A review of natural circulation loops in pressurized water reactors and other systems, Nuclear Engineering and Design 67 (1981) 203–225.

[7] A. Mertol, R. Greif, Y. Zvirin, The transient, steady state and stability behavior of a thermosyphon with throughflow, International Journal of Heat and Mass Transfer 24 (1981) 621–633.

[8] P.K. Vijayan, A.W. Date, Experimental and theoretical investigations on the steady-state and transient behavior of a thermosyphon with throughflow in a figure-of-eight loop, International Journal of Heat and Mass Transfer 33 (1990) 2479–2489.

[9] P.K. Vijayan, A.W. Date, The limits of conditional stability for single-phase natural circulation with throughflow in a figure-of-eight loop, Nuclear Engineering and Design 136 (1992) 361–380.

[10] G.B. Whitham F.R.S, Linear and Nonlinear Waves, Wiley, New York, 1974 (Chapter 2).